Table 2 Kinetic parameters

Heating rate, °C min^{-1}	Coats-Redfern			MacCallum-Tanner			Horowitz-Metzger		
	E^a	A^b	r	E^a	A^b	r	E^a	A^b	r
1	77.72	8.253×10^1	0.9979	81.17	1.568×10^2	0.9985	102.8	5.597×10^3	0.9952
2	71.70	2.612×10^1	0.9984	75.77	5.568×10^1	0.9989	96.13	1.257×10^3	0.9963
5	70.78	2.880×10^1	0.9960	75.40	6.718×10^1	0.9997	96.55	1.420×10^3	0.9989
10	66.25	2.007×10^1	09976	71.09	4.890×10^1	0.9981	93.81	1.180×10^3	0.9995
20	62.13	1.262×10^1	0.9953	67.36	3.280×10^1	0.9964	92.45	9.428×10^2	0.9994
50	57.90	1.066×10^1	0.9959	63.76	3.070×10^1	0.9971	85.60	4.388×10^2	0.9967
100	41.77	1.425×10^0	0.9804	48.20	4.671×10^0	0.9907	64.70	2.297×10^1	0.9725

(Kinetic equations)

[a]In KJ mole^{-1}. [b]In sec^{-1}.

Table 3 Curve fit constants for correlation of E and A with heating rate

Kinetic equation	Correlation with log E					Correlation with A				
	C_1	$C_2\times10^3$	$C_3\times10^5$	$C_4\times10^7$	F	K_1	$K_2\times10^{-3}$	$K_3\times10^{-3}$	$K_4\times10^{-3}$	F
Coats-Redfern	1.8832	7.2475	14.783	10.160	111.0	2.4576	0.23336	0.59131	0.43803	167.6
MacCallum-Tanner	1.9035	6.0538	12.489	8.6406	107.1	9.7077	0.52231	1.3481	0.97287	61.5
Horowitz-Metzger	2.0003	2.8251	5.0240	4.0933	63.9	131.85	13.262	36.460	28.666	148.5

best be represented by a third-degree curve, following the equation of the type

$$A = K_1 + \frac{K_2}{\phi} + \frac{K_3}{\phi^2} + \frac{K_4}{\phi^3}$$

where K_1 to K_4 are empirical constants, different for the three equations.

The reliability of the curve fittings was evaluated by the F test.[8] The values of C_1 to C_4 along with the corresponding Fisher constant F, the values of K_1 to K_4, and F for the three equations are given in Table 3. The critical value of the Fisher constant[8] for the system at 99% confidence level is 28.7. From Table 3 it can be seen that the confidence level of all the correlations is above 99%. Similar quantitative correlations between kinetic parameters and heating rate have been reported in the case of certain reactions, while for other reactions, the kinetic constants do not depend on the heating rate.[4] No universally acceptable theoretical explanation has been propounded for such systematic dependence.

Acknowledgments

The author thanks Mr. K. Krishnan for help in recording the TG curves and Mr. S. Pitchiah for help in computer programming. Thanks are also due to Dr. K.V.C. Rao, Mr. M.R. Kurup, and Dr. Vasant Gowariker for their encouragement.

References

[1]Kurwicz, H. and Rogan, J.E., "Ablation," *Handbook of Heat Transfer,* Sec. 16, edited by R.M. Rohsenow and J.P. Hartnett, McGraw-Hill Book Co., New York, 1973, pp. 49-54.

[2]Mathieu, R.D., "Response of Charring Ablators to Hyperthermal Environment," Space Science Laboratory, General Electric, R63 SD 20, Feb. 1963, pp. 9-10.

[3]Wendlandt, W.W., *Thermal Methods of Analysis,* 2nd ed., John Wiley & Sons, New York, 1974, pp. 8-36.

[4]Nair, C.G.R. and Ninan, K.N., "Thermal Decomposition Studies, Part X. Thermal Decomposition Kinetics of Calcium Oxalate Monohydrate-Correlations with Heating Rate and Sample Mass," *Thermochimica Acta,* Vol. 23, March 1978, pp. 161-169.

[5]Ninan, K.N. and Nair, C.G.R., "Thermal Decomposition Studies, Part XII. Kinetics of Dehydration of Calcium Oxalate Monohydrate. Multiple Correlation with Heating Rate and Sample Mass," *Thermochimica Acta,* Vol. 37, April 1980, pp. 161-172.

[6]Ninan, K.N. and Krishnan, K., "Thermal Decomposition Kinetics of Polybutadiene Binders," *Journal of Spacecraft and Rockets,* Vol. 19, Jan.-Feb. 1982, pp. 92-94.

[7]Zimmermann, H. and Behnisch, H., "Thermogravimetric Investigations on the Kinetics of Thermal Degradation of Polyoxymethylenes," *Thermochimica Acta,* Vol. 59, Nov. 1982, pp. 1-8.

[8]Mack, C., *Essentials of Statistics for Scientists and Technologists,* Plenum Press, New York, 1967, pp. 106-115.

Turbulent Reynolds Analogy Factors of Stacked Large-Eddy Breakup Devices

A. Margrethe Lindemann*
NASA Langley Research Center, Hampton, Virginia

Nomenclature

A	= test (flat-plate) surface area
C_f	= area-averaged skin-friction coefficient, $2D/A\rho_\infty U_\infty^2$
D	= measured total drag
h	= area-averaged heat-transfer coefficient, $Q/A(T_w/T_\infty)$
Q	= measured heat-transfer rate
Re_θ	= momentum thickness Reynolds number
T_w	= wall temperature
T_∞	= freestream temperature
U_∞	= freestream velocity
x	= streamwise distance from leading edge
δ	= boundary-layer thickness

Received Feb. 25, 1985; revision received May 18, 1985.

*Aerospace Engineer, Viscous Flow Branch, High-Speed Aerodynamics Division.

δ_{SL} = flat-plate boundary-layer thickness at future site of large-eddy breakup devices
η = Reynolds analogy efficiency factor: test surface referenced to flat plate = $(h/C_f)_{LB} \div (h/C_f)_{FP}$
ρ_∞ = freestream air density

Subscripts

FP = reference flat plate test values
LB = large-eddy breakup device (LEBU) test values

Introduction

THE current study directly measures turbulent Reynolds analogy factors (referenced to flat plate) for turbulent boundary-layer flows altered by stacked arrays of large-eddy breakup devices (LEBU), or "turbulence manipulators" or "ribbons" as they have been previously called.[1-5] LEBUs are of interest because of their drag-reducing potential. LEBU elements inserted into the boundary layer are transverse to the flow and primarily affect the outer eddy structures.[1] The net skin friction is reduced for at least 120 δ_{SL} downstream of these devices.[2] The measured Reynolds analogy factors provide quantitative information concerning the heat-transfer characteristics associated with these altered boundary layers. Test momentum thickness Reynolds numbers (midplate values) range in two groups of 2000-3100 and 4000-6400. Both groups span the same speed range and experimental conditions, differing only in the origin of their turbulence. The lower Reynolds numbers are associated with two-dimensional rod trips, the higher Reynolds numbers with three-dimensional swept screen trips. The data, which have also been examined in the context of these distinct trips and Reynolds numbers, provide evidence that heat transfer, skin-friction drag, and LEBU performance factors in these low Reynolds number flows are sensitive to flow history.

Apparatus and Measurement Procedures

Heat-transfer and drag measurements were obtained in a Langley low-speed wind tunnel that has a 91.4 cm long test section with a cross section 17.8 cm high × 27.9 cm wide. Refer to Table 1 for information concerning test boundary-layer parameters, LEBU configurations, and trip descriptions. The flat aluminum plate test surface, 1.27 cm thick × 91.4 cm long × 27.9 cm wide, comprises the tunnel test section floor. Each of the respective trips was installed 25.4 cm upstream of the flat-plate leading edge; the LEBUs were longitudinally located 5.08 cm downstream from the leading edge. Heat-transfer and drag measurements for the flat-plate references and for the LEBU stacks were made at each of three speeds: 19.8, 27.4, and 36.6 m/s.

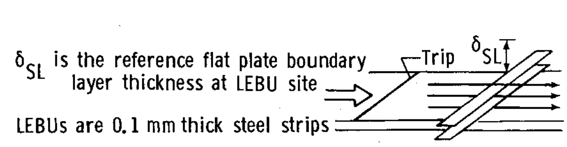

Fig. 1 Two-LEBU stack.

The LEBUs were implemented in stacked configurations. See Refs. 1, 2, 5, and 6 for detailed descriptions of similar setups and the LEBU design. The LEBUs were tautly strung above and transverse to the flat test surface in three-stack (0.3, 0.6, and 0.9 δ_{SL}); two-stack (0.4 and 0.8 δ_{SL}) and one-stack (0.6 δ_{SL}) arrays. Figure 1 is a simplified schematic diagram of a two-LEBU stack. Care was taken in mounting the LEBUs to eliminate vibration, twisting, slipping, or deviation from zero angle of attack (i.e., parallel to the wall).

Heat-transfer coefficients for the test configurations were determined using the Newton convective heat-transfer equation for low-speed airflow,

$$Q = Ah(T_w - T_\infty)$$

The flat plate in each test configuration was heated with a common heater element designed and instrumented to provide a steady-state heat output following correction for conduction, radiation, and storage. A surface array of temperature measurements derived from a distribution of 11 thermocouples (embedded 0.19 cm below the test surface) provided the area ΔT distribution (nominally 5°C above ambient). The heat-transfer measurements were repeatable to within ±2%. More complete heat-transfer measurement procedural details may be found in Ref. 7.

Drag measurements utilized a free-floating air bearing drag balance, which necessitated maintaining slight (0.076 cm) gaps about the perimeter of the tests surface. (These same gaps were duplicated in the heat-transfer setup.) In order to

Table 2 Test data

No. of LEBUs	U_∞, m/s	h_{LB}/h_{FP}	$C_{f_{LB}}/C_{f_{FP}}$	η
		Rod trip		
3	19.8	0.99	0.89	1.11
	27.4	0.94	0.93	1.01
	36.6	0.94	0.90	1.04
2	19.8	1.13	0.95	1.19
	27.4	1.04	0.95	1.10
	36.6	1.04	0.95	1.09
1	19.8	1.12	0.99	1.14
	27.4	1.03	0.97	1.07
	36.6	0.93	0.98	0.95
		Swept screen trip		
3	19.8	0.97	0.87	1.12
	27.4	0.92	0.87	1.06
	36.6	0.93	0.87	1.07
2	19.8	0.97	0.90	1.08
	27.4	1.00	0.90	1.10
	36.6	0.95	0.89	1.08
1	19.8	1.04	0.97	1.07
	27.4	0.98	0.96	1.02
	36.6	0.97	0.94	1.03

Table 1 Boundary-layer and LEBU parameters

Trip	LEBU chord, cm	U_∞, m/s	5.1 cm downstream leading edge: δ_{SL}, cm	5.1 cm downstream leading edge: Re_θ	66 cm downstream leading edge: δ, cm	66 cm downstream leading edge: Re_θ
Two-dimensional rod,	0.8	19.8	1.22	1400	1.89	2575
0.15 cm diam	0.8	27.4	1.15	1760	1.69	3060
	0.8	36.6	1.03	2200	1.72	4075
Three-dimensional	1.20	19.8	1.75	3610	3.05	4525
(wire) screen	1.20	27.4	1.63	4480	2.75	5356
2.54 cm long	1.20	36.6	1.59	5750	2.74	6990
at 15 deg						

minimize blowing and suction at the gaps, both drag and heat-transfer tests operated a vacuum system in the plenum chamber enclosing the test section in order to match the static pressure below the drag balance or heater plate support with that of the test section. The rear side wall was adjusted in both sets of measurements to actively maintain a near-zero pressure gradient in the test section. Careful model alignment and calibration checks insured drag data repeatability to within ±1%. Skin-friction coefficients were backed out from direct drag measurements using the following relation:

$$D = \tfrac{1}{2} A C_f \rho_\infty U_\infty^2$$

Results and Discussion

The LEBU heat-transfer coefficients were generally depressed (6% maximum reduction) below flat-plate values. See Table 2 for test heat-transfer data. The three-LEBU stacks produced the lowest heat-transfer coefficients for the two sets of tripped flows. As U_∞ and Re_θ increase, the test heat-transfer coefficients for a given stack configuration decrease, while the flat-plate reference coefficients remain stable throughout the test speed range. In fact, all flat-plate heat-transfer coefficients for both rod and screen trips were roughly equivalent to within experimental error. It is particularly interesting to note that if the scatter in the screen-tripped heat-tansfer data were merely a phenomenon of experimental error, then it does not appear that the screen-tripped heat-transfer data were a function of velocity. In contrast, while the rod-tripped heat-transfer data are monotonic, that data may well be velocity- and/or Re_θ-dependent (lower Re_θ, post-transitional flow).

Drag data for the LEBUs agree in trend to previous data in similar configurations and test conditions.[1,2,6] (See Table 2 for test drag data.) The three-LEBU stack yielded average C_f reductions of up to 13% (screen trip only) and consistently exhibited the greatest average C_f reductions of all the LEBU configurations for both sets of tripped flows. (Note that the recorded experimental average C_f reductions do not include the penalty of device drag.) The reductions associated with the screen trip and higher Reynolds numbers are significantly greater than with the two-dimensional rod trip (transitional flow effects[2]). Note that, unlike the heat-transfer cases, the drag results remain markedly stable for a given configuration throughout the test speed range.

Because the overall C_f reductions exceed the heat-transfer coefficient reductions, the relative Reynolds analogy factors (here constructed in terms of the simple efficiency relation η) are somewhat increased above (average increase approximately 7%) the appropriate flat-plate reference. Again refer to Table 2 for measured relative LEBU Reynolds analogy factors. The two-LEBU stacks exhibit the highest Reynolds analogy factors for both sets of tripped flows. Reynolds analogy factors tend to decrease as U_∞ increases per each LEBU stack; other trends, if any, are difficult to identify.

The fact that LEBUs heat transfer is reduced is not surprising for several reasons: LEBUs tend to reduce the vertical component (primary heat-transfer direction) of large-scale motion[1] and insertion of LEBUs causes a redistribution of fine-scale turbulence in place of large, more uneven structures (inherently better carriers of thermal energy differentials).[2] Reynolds analogy factors for LEBUs, however, are generally elevated above flat-plate values, which means that the C_f reduction is greater than the corresponding heat-transfer reduction. This suggestion also makes sense in the light of such experimental observations that: 1) the wall law similarity is re-established early for $y/\delta_{SL} > 0.3$, (i.e., forecasting nominal heat-transfer reduction), although C_f reductions persist;[3] and 2) for 30% LEBU C_f reduction, the sublayer is increased 17% (i.e., turbulent heat-transfer reduction conceivably closer to 17%).

In addition to the above results, the variation in stability of the LEBU heat-transfer and skin-friction data throughout the test speed range also suggests that independent mechanisms influence the two flow parameters. In support of this interpretation, a growing body of experimental data offers evidence that, contrary to the similarity imposed by standard Reynolds analogy models, heat transfer and skin friction are affected differently in situations characterized by surface roughness or curvature, physical or thermal steps, and pressure gradients.

References

[1]Corke, T.C., Nagib, H.M., and Guezennec, Y.G., "A New View on Origin, Role and Manipulation of Large Scales in Turbulent Boundary Layers," NASA CR-165861, Feb. 1982.

[2]Anders, J.B., Hefner, J.N., and Bushnell, D.M., "Performance of Lage-Eddy Breakup Devices at Post-Transitional Reynolds Numbers," AIAA Paper 84-0345, Jan. 1984.

[3]Nguyen, V.D., Dickinson, J., Lemay, A.J., Haeberle, D., Larose, G., Boisvert, L.M., Chalifour, Y., and Jean, Y., "Some Experimental Observations of the Law of the Wall Behind Large-Eddy Breakup Devices Using Servo-Controlled Skin Friction Balances," AIAA Paper 84-0346, Jan. 1984.

[4]Nguyen, V.D., Dickinson, J., Lemay, J., Provencal, D., Jean, Y., and Chalifour, Y., "The Determination of Turbulent Skin Friction Behind Flat Plate Turbulence Manipulators Using Servo-Controlled Balances," *Proceedings of the International Council of the Aeronautical Sciences Congress XIV,* Vol. 1, 1984, pp. 404-409.

[5]Mumford, J.C. and Savill, A.M., "Parametric Studies of Flat Plate, Turbulence Manipulators Including Direct Drag Results and Laser Flow Visualization" *Laminar and Turbulent Boundary Layers, Proceedings of the Energy Sources Technology Conference,* Rolls Royce, 1984, pp. 41-51.

[6]Bandyopadhyay, P.R., "The Performance of Smooth-Wall Drag Reducing Outer-Layer Devices in Rough-Wall Boundary Layers," AIAA Paper 85-0558, March 1985.

[7]Lindemann, A.M., "Turbulent Reynolds Analogy Factors for Nonplanar Surface Microgeometries," *Journal of Spacecraft and Rockets,* Vol. 22, Sept.-Oct. 1985, pp. 581-582.

Analyses of Spacecraft Polymeric Materials

S. D. Worley,* C. H. Dai,† J. L. Graham,†
A. T. Fromhold,† and K. Daneshvar§
Auburn University, Auburn, Alabama
and
A. F. Whitaker¶ and S. A. Little**
Marshall Space Flight Center, Huntsville, Alabama

Introduction

It has been recognized since the pioneering work of Leger[1] concerning materials exposed on missions STS-1 through STS-3 and of Hansen and coworkers[2] in a ground-based study that LEO atomic oxygen may present a serious problem for materials used in conjuction with the space telescope. Atomic oxygen is the major ambient species at low orbital altitudes and presents a flux of *ca.* 8×10^{14} atoms cm^{-2} s^{-1} for oxidative reaction with materials.[1] Leger observed a significant alteration in appearance of the Kapton

Received Aug. 2, 1985; revision received Dec. 16, 1985.

*Alumni Professor of Chemistry.

†Graduate Student, Chemistry.

‡Professor of Physics.

§Assistant Professor of Electrical Engineering.

¶Deputy Chief, Engineering Physics Division. Member AIAA.

**Physicist, Physical Sciences Branch.